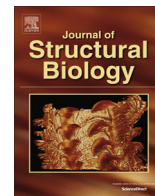




Contents lists available at ScienceDirect

Journal of Structural Biology

journal homepage: www.elsevier.com/locate/yjsbi

Imaging complement by phase-plate cryo-electron tomography from initiation to pore formation

Thomas H. Sharp^{a,*}, Frank G.A. Faas^a, Abraham J. Koster^{a,b}, Piet Gros^{c,*}

^a Section Electron Microscopy, Department of Molecular Cell Biology, Leiden University Medical Center, 2300 RC Leiden, The Netherlands

^b NeCEN, Gorlaeus Laboratories, Leiden University, 2333 CC Leiden, The Netherlands

^c Crystal and Structural Chemistry, Bijvoet Center for Biomolecular Research, Department of Chemistry, Faculty of Science, Utrecht University, Padualaan 8, 3584 CH Utrecht, The Netherlands

ARTICLE INFO

Article history:

Received 24 May 2016

Received in revised form 17 August 2016

Accepted 13 September 2016

Available online xxxxx

Keywords:

C1

Complement

Electron tomography

Membrane attack complex

Phase plate

ABSTRACT

Phase plates in cryo-electron tomography (cryoET) improve contrast, increasing the ability to discern separate molecules and molecular complexes in dense biomolecular environments. Here, we applied this new technology to the activation of the human complement system. Binding of C1 to antigen-antibody complexes initiates a cascade of proteolytic events that deposits molecules onto adjacent surfaces and terminates with the formation of membrane-attack-complex (MAC) pores in the targeted membranes. We imaged steps in this process using a Volta phase plate mounted on a Titan Krios equipped with a Falcon-II direct electron detector. The data show patches of single-layer antibodies on the surface and C1 bound to antibody platforms, with ca. ~4% of instances where C1r and C1s proteases have dissociated from C1, and potentially instances of C1 transiently interacting with its substrate C4 or product C4b. Next, extensive deposition of C4b and C3b molecules is apparent, although individual molecules cannot always be properly distinguished with the current methods. Observations of MAC pores include formation of both single and composite pores, and instances of potential soluble-MAC dissociation upon failure of membrane insertion. Overall, application of the Volta phase plate cryoET markedly improved the contrast in the tomograms, which allowed for individual components to be more readily interpreted. However, variability in the phase shift induced by the phase-plate during the course of an experiment, together with incomplete sampling during tomogram acquisition, limited the interpretability of the resulting tomograms. Our studies exemplify the potential in studying molecular processes with complex spatial topologies by phase-plate cryoET.

© 2016 Elsevier Inc. All rights reserved.

1. Introduction

Cryo-electron tomography (cryoET) allows three-dimensional imaging of macromolecular structures up to several hundred nm in size yet with nm-scale resolution (Asano et al., 2016). In recent years, significant improvements of the instrumentation required for cryo-electron microscopy (cryoEM) have become available, in particular direct-electron detectors, highly stable cryo-electron microscopes, and the capacity for multi-day data collection (Cheng, 2015). Nevertheless, cryoEM inherently suffers from suppressed image contrast at low spatial frequencies that can only

be partly restored by defocusing, which leads to reduced resolution (Erickson and Klug, 1971). Recently a phase plate (the Volta phase plate; VPP) became commercially available for cryoEM, which restores the low-frequency contrast (Danev et al., 2014), allowing in-focus data collection and single-particle analysis (Danev and Baumeister, 2016; Khoshouei et al., 2016b), cryoET (Fukuda et al., 2015), and subtomogram averaging (Asano et al., 2015; Sharp et al., 2016). The resolution of cryo-tomograms, and subsequent sub-tomogram averages, is limited by frequency-dependent contrast reversals as described by the contrast transfer function (CTF) (Fernandez et al., 2006; Xiong et al., 2009). However, with a phase plate the need to generate low-frequency contrast by defocusing is no longer required, with the consequence that the frequency of the first contrast reversal is increased with respect to cryoET without a phase plate (Danev and Nagayama, 2001). This results in higher resolution tomograms with more contrast, facilitating their direct interpretation without subtomogram averaging

Abbreviations: CC, correlation coefficient; cryoEM/T, cryo-electron microscopy/tomography; CTF, contrast transfer function; DNP, 2,4-dinitrophenyl; FB, factor B; MAC, membrane attack complex; NHS, normal human sera/serum; VPP, Volta phase plate.

* Corresponding authors.

E-mail addresses: t.sharp@lumc.nl (T.H. Sharp), p.gros@uu.nl (P. Gros).

<http://dx.doi.org/10.1016/j.jsb.2016.09.008>

1047-8477/© 2016 Elsevier Inc. All rights reserved.

(Fukuda et al., 2015). Recently, we applied phase-plate cryoET in combination with subtomogram averaging to visualize formation of the membrane-attack complex (MAC), the final stage of the complement pathway (Sharp et al., 2016). Herein, we use electron cryo-tomograms collected using a VPP to study the molecular distribution of complement components on synthetic cell mimics, and visualize the development of complement activation using depleted sera to block the linear cascade at discrete stages.

The mammalian complement system provides protection against invading microbes in blood or interstitial fluids by labeling them for destruction and induction of immune-cell responses, such as phagocytosis by macrophages and stimulation of B and T cells. The pathways of complement have been extensively reviewed, see e.g. (Bajic et al., 2015; Dunkelberger and Song, 2010; Merle et al., 2015a,b; Ricklin et al., 2010; Walport, 2001). In brief, the complement system consists of ca. 30 soluble plasma proteins and cell-surface receptors. In the presented study we focused on the plasma proteins of the complement system reacting with lipid bilayer surfaces, using synthetic liposomes as a model system (Yamamoto et al., 1995). Specifically, the classical pathway of complement activation is initiated on these liposomes by binding of antibodies to lipid-bound haptens, forming immune complexes on the liposome membrane. Next, the first complement component C1, a 790-kDa complex consisting of a hexameric recognition module C1q and a hetero-tetramer of proteases C1r and C1s, binds to the immune complexes, starting the proteolytic cascade of complement. The activated proteases C1s in C1 cleave both C4 and C2 forming a C4b2a complex (where “b” and “a” indicate cleavage products), which in turn cleaves C3 producing C3b. The homologous products C4b and C3b attach to the targeted microbes *via* reactive thioester moieties, which become exposed upon cleavage of C4 and C3, and covalently react with hydroxyl- and amino-groups on the microbial surface. This labeling, or opsonization, of the microbe is enhanced through a positive feedback loop in which protease factor B (FB) binds to C3b and is cleaved by factor D forming a C3bBb complex. This loop may also initiate complement via spontaneous hydrolysis of C3, known as the alternative pathway. Both C4b2a and C3bBb are C3 convertases, but additional deposition of C3b molecules can yield ternary complexes C4b3b2a and C3b₂Bb, which alter their substrate specificity from C3 to C5, hence forming C5 convertases. Cleavage of C5 marks the terminal pathway of complement activation. C5b associates with C6, C7, C8 and multiple copies of C9 forming the membrane-attack-complex (MAC), large ~100-Å wide pores, which lyse the microbial membrane.

Two previous papers (Diebolder et al., 2014; Sharp et al., 2016) demonstrated the potential of our model system for imaging complement initiation and MAC-pore formation. Here, we will report further results obtained in our efforts to provide a step-by-step visualization of complement activation on a membrane surface. These studies illustrate the major advances in cryoET using the recent technical developments, reveal its current limitations, and indicate the potential of imaging complex biological processes using cryoET.

2. Materials and methods

2.1. Complement activity assays

Purified protein, depleted sera and normal human sera (NHS) were purchased from Complement Technologies (Complement Technologies, Texas, USA) and stored at -80 °C. For complement activity assays, 2,4-dinitrophenyl (DNP)-labeled liposomes (Wako Diagnostics, Virginia, USA) were monitored at 340 nm using an Ultrospec 2100 pro (Biochrom Ltd., Cambridge, UK), as described

(Yamamoto et al., 1995). Sera were used at final concentrations of 2.5 vol%. Depleted sera were reconstituted with the respective purified protein at the following concentrations prior to assay: C2, 0.02 mg/ml; C4, 0.4 mg/ml; C3, 1.2 mg/ml; C5, 0.075 mg/ml (Morley and Walport, 2000).

2.2. Cryo-electron tomography

Liposomes were mixed with antibodies and sera as described above and vitrified as described in (Sharp et al., 2016). A Tecnai T20 (FEI Company, Eindhoven, NL) equipped with a field emission gun operating at 200 kV was used to acquire tilt series without a phase plate, which were imaged at $\times 29$ k magnification on a Gatan Ultrascan 4 k charged coupled device (Gatan, Inc., Abingdon, UK) binned $2\times$, for a final pixel size of 0.79 nm, using a tilt scheme from -60° to $+60^\circ$ in 2° increments. Focussing to -6000 nm was performed prior to each image acquisition using low-dose conditions. The total dose for each tomogram was ~ 6100 e^-/nm^2 . Tilt-series collected with the phase plate were acquired using a Titan Krios transmission electron microscope (FEI Company, Eindhoven, NL) equipped with a field emission gun operating at 300 kV. Alignment of beam-shift pivot points and on-plane illumination was performed prior to imaging. A Volta phase plate (FEI, Eindhoven, The Netherlands), heated to 225 °C, was conditioned for 300 s with a dose of 0.17 nA for a final charge of ca. 50 nC to generate an approximate phase shift of 90° . The VPP was advanced to a new area before the acquisition of each tilt series, and allowed to settle for 300 s before re-conditioning. The phase plate was also conditioned for an additional 10 s between each tilt image. Discontinuous tilt series were collected using Tomography 4.0 (FEI Company, Eindhoven, The Netherlands) at $\times 29$ k magnification using a tilt scheme from 0° to -60° before collecting 0° to $+60^\circ$, in 2° increments. Total dose for the tilt series was 6100 e^-/nm^2 . Focusing to -500 nm was performed prior to each image acquisition using a low-dose routine.

2.3. Tomogram processing

Tomograms were semi-automatically processed with batchrun-tomo from the software program IMOD (Mastrorarde and Held, 2016) using fiducial-based tracking methods. For tilt series acquired without the phase plate, CTF determination was performed using the software program TomoCTF (Fernandez et al., 2006) and corrected using ctfphaseflip within IMOD (Xiong et al., 2009). For tilt series acquired with the phase plate, no CTF correction was performed. Gold fiducials were erased after alignment prior to reconstruction. Tomograms were reconstructed using eight iterations of the simultaneous iterative reconstruction technique (SIRT).

Electron microscopy density maps EMD-2507 (Diebolder et al., 2014) and EMD-3289 (Sharp et al., 2016) were used for C1 and the MAC pore, respectively. Maps were fit into tomogram volumes using the “fit-in-map” routine from UCSF Chimera (Pettersen et al., 2004). Isosurfaces representations were de-noised for clarity by hiding disconnected particles smaller than 2000 voxels using the command “hide dust” within UCSF Chimera. Particles were colored by correlation coefficient (CC), and colors were normalized to the highest CC in each tomogram from blue (highest) to red (CC = 0): since the missing wedge is present in tomograms but not in subtomogram averages the maximum CC did not achieve unity. The C1s domains were modeled using crystal structure 4J1Y (Perry et al., 2013) and manually oriented in the tomograms. All images and movies were made with UCSF Chimera (Pettersen et al., 2004).

Download English Version:

<https://daneshyari.com/en/article/5591553>

Download Persian Version:

<https://daneshyari.com/article/5591553>

[Daneshyari.com](https://daneshyari.com)